An Increased Intraovarian Synthesis of Nerve Growth Factor and Its Low Affinity Receptor Is a Principal Component of Steroid-Induced Polycystic Ovary in the Rat*

H. E. LARA, G. A. DISSEN, V. LEYTON, A. PAREDES, H. FUENZALIDA, J. L. FIEDLER, AND S. R. OJEDA

Laboratory of Neurobiochemistry, Faculty of Chemistry and Pharmaceutical Sciences (H.E.L., A.P., J.L.F.), and Faculty of Medicine (V.L., H.F.), Universidad de Chile, Santiago, Chile; and the Division of Neuroscience, Oregon Regional Primate Research Center/Oregon Health Sciences University (G.A.D., S.R.O.), Beaverton, Oregon 97006

ABSTRACT

A form of polycystic ovary (PCO) resembling some aspects of the human PCO syndrome can be induced in rats by a single injection of estradiol valerate (EV). An increase in sympathetic outflow to the ovary precedes, by several weeks, the appearance of cysts, suggesting the involvement of a neurogenic component in the pathology of this ovarian dysfunction. The present study was carried out to test the hypotheses that this change in sympathetic tone is related to an augmented production of ovarian nerve growth factor (NGF), and that this abnormally elevated production of NGF contributes to the formation of ovarian cysts induced by EV. Injection of the steroid resulted in increased intraovarian synthesis of NGF and its low affinity receptor, p75 NGFR. The increase was maximal 30 days after EV, coinciding with the elevation in sympathetic tone to the ovary and preceding the appearance of follicular cysts. Intraovarian injections of the retrograde tracer fluorogold combined with *in situ* hybridization to detect tyrosine hydroxylase (TH) messenger RNA-containing neurons in the celiac ganglion revealed that these changes in NGF/p75 NGFR synthesis are accompanied by selective activation of noradrenergic neurons projecting to the ovary. The levels of RBT_2 messenger RNA, which encodes a β-tubulin presumably involved in slow axonal transport, were markedly elevated, indicating that EV-induced formation of ovarian cysts is preceded by functional activation of celiac ganglion neurons, including those innervating the ovary. Intraovarian administration of a neutralizing antiserum to NGF in conjunction with an antisense oligodeoxynucleotide to p75 NGFR, via Alzet osmotic minipumps, restored estrous cyclicity and ovulatory capacity in a majority of EV-treated rats. These functional changes were accompanied by restoration of the number of antral follicles per ovary that had been depleted by EV and a significant reduction in the number of both precystic follicles and follicular cysts. The results indicate that the hyperactivation of ovarian sympathetic nerves seen in EV-induced PCO is related to an overproduction of NGF and its low affinity receptor in the gland. They also suggest that activation of this neurotrophic-neurogenic regulatory loop is a component of the pathological process by which EV induces cyst formation and anovulation in rodents. The possibility exists that a similar alteration in neurotrophic input to the ovary contributes to the etiology and/or maintenance of the PCO syndrome in humans.

IT IS now clear that ovarian function is regulated by both hormonal and intraovarian signals acting in synchrony to control follicular development, steroid secretion, and ovulation. In recent years, evidence has accumulated indicating that the sympathetic innervation of the ovary also contributes to this regulatory process by facilitating both follicular development (1, 2) and ovarian steroidogenesis (3, 4).

Studies using a rodent model of the human syndrome of polycystic ovary (5) first suggested that an alteration in peripheral sympathetic activity may contribute to the etiology and/or progression of cystic ovarian disease. Polycystic ovarian syndrome (PCOS) is a complex disease characterized by ovulatory failure, amenorrhea, hyperandrogenemia, and variable levels of circulating gonadotropins (6, 7). PCOS is widely recognized as the most common cause of infertility in women. To date, the precise etiology of the disease remains unknown, even though it appears clear that its initiation and progression may be determined by a variety of interrelated factors (6, 7). The abnormalities detected in PCOS have been attributed to primary defects in the hypothalamic-pituitary unit, the ovarian microenvironment, the adrenal gland, and the insulin/insulin-like growth factor I metabolic regulatory system (7, 8). A very recent study used genetic linkage analysis to search for loci contributing to PCOS and identified follistatin as the gene product with the strongest linkage to the disorder (9). Despite this multiplicity of potential etiologies, a feature common to most forms of PCOS is the lack of dominant preovulatory follicles, which are replaced by multiple medium-size antral follicles containing an enlarged, androgen-producing, thecal layer (10).

The potential contribution of the peripheral sympathetic system to the syndrome has been suggested by several observations, including the increased density of catecholaminergic nerves detected by histofluorescence in patients suf-

Address all correspondence and requests for reprints to: Dr. Sergio R. Ojeda, Division of Neuroscience, Oregon Regional Primate Research Center, 505 NW 185th Avenue, Beaverton, Oregon 97006.

* This work was supported by the Fondo Nacional de Ciencias de Chile (Project 1961018) and The Rockefeller Foundation (to H.E.L.) and by NIH Grants HD-24870 (to S.R.O.), and P30 Population Center Grant HD-18185 and RR-00163 for the operation of the Oregon Regional Primate Research Center.

fering from the disease (11) and the effectiveness of ovarian wedge resection to restore ovulatory capacity, especially when it compromises the hilum (12, 13), the point of entry of nerves into the ovary. That PCOS may indeed be associated with an abnormal activation of the sympathetic nervous system is indicated by the results of a recent report showing an impaired metabolism of norepinephrine (NE) in adolescents suffering from the disease (14). Rats injected with a single dose of estradiol valerate (EV) develop an anovulatory condition that resembles in several, but not all, aspects the human syndrome (15). Using this rodent model, we demonstrated (5) that the appearance of ovarian cysts after EV administration is preceded by an increased activity of the sympathetic nerves arriving at the ovary via the superior ovarian nerve (SON). The SON carries the bulk of the noradrenergic innervation to the secretory cells of the ovary (16). Its transection in EV-treated rats resulted in restoration of cyclicity and ovulatory capacity (17), indicating that hyperactivation of the ovarian sympathetic nerves plays an important role in maintaining the EV-induced anovulatory condition.

The development and function of the ovarian sympathetic innervation depend on the ability of the ovary to produce nerve growth factor (NGF) (1), a target-derived neurotrophin required for the development of the peripheral sympathetic system (18). In the rat ovary, NGF is preferentially synthesized in cells of the follicular wall (19), which is a terminal field for the sympathetic neurons projecting to the ovary (1, 16). Transfer of NGF from its sites of production to the innervating fibers has been postulated to occur via binding of the neurotrophin to the low affinity neurotrophin receptor (20), known as p75 NGF receptor (p75 NGFR or p75 NTR). Thus, activation of this target-derived trophic system may be a factor involved in enhancing NE outflow to the gland in the EV-induced polycystic ovary. The results of the present study are consistent with this concept. They further indicate that an augmented intraovarian production of NGF and its low affinity receptor is an important component of the process by which follicular cysts, acyclicity, and anovulation are maintained in EV-treated rats. A preliminary report of these findings has appeared in abstract form (21).

Materials and Methods

Animals

Virgin adult cycling rats of the Sprague Dawley strain, weighing 200–220 g, were used. The animals were kept on a 14-h light, 10-h dark photoperiod (lights on from 0500–1900 h) and allowed free access to pelleted rat chow and tap water. Animals showing at least two regular 4-day cycles were selected for the experiments. A PCO condition was induced by the administration of EV (Sigma, St. Louis, MO) as a single im injection (2 mg/rat diluted in 0.2 ml corn oil) as previously reported (5, 22). Control rats were injected with oil. Different groups of animals were analyzed at several intervals after the injection (7, 15, 30, and 60 days). The 60-day interval was chosen as the last time point, because it corresponds to the time when the cysts become clearly established (23).

Measurement of tyrosine hydroxylase (TH) activity

To measure TH activity in the celiac ganglion, the main source of sympathetic fibers reaching the ovary via the SON (24), the ganglion was excised (along with adjacent tissue) from its location between the abdominal aorta and the superior mesenteric and celiac arteries, as described by Lawrence and Burden (16). The enzyme activity was determined by the method of Waymire *et al.* (25), as previously described (26). The procedure involves measuring the $^{14}CO_2$ released from 1-[^{14}C]tyrosine (SA, 52 mCi/mmol; NEN Life Science Products, Boston, MA) after hydroxylation by endogenous TH, followed by DOPA decarboxylase-mediated decarboxylation. The source of DOPA decarboxylase was a crude extract from pig kidneys. Tissues were first homogenized in 10 vol 0.1 M acetate buffer (pH 6.1) and 0.1% Triton X-100. The homogenates were centrifuged at 20,000 $\times$ *g* for 10 min, and the supernatants were used as samples. The assay was performed in the presence of a saturating concentration of 1 mM 6-methyl-tetrahydrobiopterin (Sigma) as a cofactor for TH. The enzymatic activity is expressed as nanomoles of CO_2 formed per 30 min.

Ribonuclease (RNase) protection assay

This assay was employed to measure the content of TH and class IV β-tubulin messenger RNA (mRNA) in the celiac ganglion and that of NGF and its low affinity receptor p75 NGFR mRNA in the ovary. The procedure used has been described in detail previously (27). A TH complementary DNA (cDNA) corresponding to nucleotides (nt) 1241–1521 in rat TH mRNA (28) was subcloned into the riboprobe vector pGEM-3Z, linearized with *Hin*dIII, and used as a template to synthesize a 280-nt [^{32}P]UTP-labeled TH antisense RNA probe. To determine whether EV affects cytoplasmic transport in celiac ganglion neurons, we measured the changes in mRNA encoding class IV β-tubulin (RBT_2). Synthesis of this tubulin subunit in the nervous system of the rat increases after the major phase of neuronal differentiation and growth has ended (29), and thus it may be more relevant to microtubule functions related to axonal transport than to neurite elongation (29, 30). The RBT_2 DNA template used for transcription (subcloned into the riboprobe vector SP64) spans 240 bp of the 3′-untranslated region of class IV β-tubulin mRNA (29). Linearization of the plasmid with *Eco*RI and use of SP6 polymerase as the enzyme for transcription yielded the antisense RNA used for the assay. To prepare an NGF complementary RNA (cRNA) probe, a 771-bp NGF cDNA was subcloned into pGEM-3Z, linearized with *Tth*III1, and used to synthesize a 324-nt antisense probe complementary to nt 702-1025 in rat NGF mRNA (31). In the case of p75 NGFR mRNA, the DNA template was a 277-bp cDNA subcloned in pGEM-3Z and linearized with *Ava*I. SP6 polymerase-directed transcription yielded a 275-bp antisense RNA probe, complementary to nt 430–705 in rat p75 NGFR (32). In each case, standards for mRNA quantitation were prepared from sense mRNAs transcribed from the same DNA templates used for the preparation of cRNAs, but in the opposite direction.

The tissue RNA samples (10–25 μg) and the RNA standards were hybridized to 500,000 cpm labeled probe for 15–17 h at 45 C. To correct for procedural variabilities, the RNA samples were simultaneously hybridized to a cyclophilin cRNA probe that recognizes the constitutively expressed cyclophilin gene (33). Cyclophilin mRNA levels remain unchanged throughout postnatal ovarian development (19, 34) and thus provide an adequate internal control for normalization of changes that may occur in the content of the mRNA of interest. The cyclophilin cRNA used is complementary to nt 338–469 in rat cyclophilin mRNA (33). After hybridization, the samples were treated with RNase A plus T1 to digest nonhybridizing species, and the protected fragments were isolated in a 5% polyacrylamide-7 M urea gel. After exposure to Kodak XAR-5 film (Eastman Kodak Co., Rochester, NY) at −85 C, the autoradiographic signals were analyzed using an Agfa (Agfa, Bertronge, Belgium) flatbed scanner and the computer program NIH Image, as previously reported (19).

Combined in situ hybridization and retrograde fluorescent tracing

This procedure was employed to determine whether the formation of cysts induced by EV treatment is preceded by an increase in TH gene expression in catecholaminergic neurons projecting from the celiac ganglion to the ovary. Thirty days after EV injection, 3 μl of a 5% fluorogold (Fluochrome, Englewood, CO) solution dissolved in 0.1 M cacodylic acid were pressure-injected into several sites of the ovary of brevital-anesthetized animals. Both oil-injected (n = 3) and EV-treated rats (n = 3) were similarly treated. In two additional animals, the fluorogold was

injected after section of the ovarian nerves. After the injection, the site of needle entry was sealed with a drop of superbonder (cyanoacrylate), and the ovary was returned to the peritoneal cavity. Ten days later, the ipsilateral celiac ganglion was dissected and fixed by immersion in 4% paraformaldehyde-borate buffer, pH 9.5, for 18–20 h at 4 C (35). Thereafter, the tissues were immersed in 10% sucrose in PBS for 24 h and frozen in OCT compound (Miles, Elkhart, IN), before cryostat sectioning. Ten-micron sections were then hybridized, as previously described (36), with a solution containing 1×10^7 cpm/ml of a [^{35}S]UTP-labeled TH cRNA probe. After hybridization at 55 C for 18–20 h and washes to a final stringency of 0.1 × SSC at 65 C for 30 min, the sections were defatted and dipped in NTB-2 emulsion. Ten days later, the reactions were developed, and fluorogold-containing neurons were identified under a fluorescence microscope equipped with darkfield illumination, using bands of UV excitation (emission maximum, 408 nm; excitation maximum, 323 nm), as previously recommended (37). Only sections containing fluorogold-labeled neurons (at least three sections per ganglion) were analyzed; microscopic images were photographed and digitized for computer analysis, as previously reported (38). In brief, background levels and individual grain size were first determined for each slide. The grains over each neuron were then identified, captured, and digitized. The number of grains per cell were calculated from the number of positive digitized pixels, using as a reference the average grain size, and the predetermined background density as a correction factor. Neurons were considered positive when the corrected number of grains exceeded the background density by a factor of 3. By estimating the TH mRNA content in individual ganglion cells (as assessed by the number of silver grains per cell) and identifying those cells containing fluorogold (*i.e.* those that project to the ovary), it was possible to assess differences in TH mRNA levels between cells innervating the ovary and those sending their axons elsewhere.

NGF two-site immunoassay and determination of p75 NGFR protein content by cross-linking to [^{125}I]NGF

Ovarian NGF content was measured by a highly sensitive two-site fluorometric enzyme immunoassay (39), exactly as previously described (40). Detection of p75 NGFR protein was achieved by cross-linking [^{125}I]NGF to ovarian membranes, followed by immunoprecipitation of the NGF-p75 NGFR complex with a monoclonal antibody (192 IgG) directed against the receptor (41) and separation of the cross-linked species by SDS-PAGE. The procedure employed has been described in detail previously (42).

Intraovarian administration of NGF antibodies and antisense oligodeoxynucleotides to p75 NGFR mRNA

Rats were injected with EV as before and immediately implanted sc with an Alzet miniosmotic pump (model 2ML4, Alza Corp., Palo Alto, CA) loaded with a mixture of polyclonal NGF antibodies (diluted 1:100) to block NGF biological actions (1, 19), and a p75 NGFR mRNA antisense phosphothionate oligodeoxynucleotide (5 μM) to reduce p75 NGFR synthesis (43). This mixture is henceforth referred to as NGF Ab + p75 NGFR AS. The oligonucleotide (5′-AGT-GGA-CTC-GCT-GCA-TAG-3′) is directed against the 3′-region of NGFR mRNA and has been shown to effectively block p75 NGFR synthesis (43). Control animals were infused with preimmune serum (PIMS). As the treatment was instituted to restore ovarian function, rather than to disrupt it, control animals were not infused with a p75 NGFR scrambled oligonucleotide sequence. Such a sequence has been previously shown to be ineffective in reproducing the inhibitory effect of p75 NGFR AS on kidney development (43).

The osmotic pump was connected to SILASTIC brand tubing (Dow Corning Corp., Midland, MI; id, 0.020 in.; od, 0.037 in.), which was then inserted underneath the bursa of the left ovary and kept in place by a drop of cyanoacrylate and sutures attached to the ipsilateral uterine horn. Delivering a flow rate of 2.5 μl/min, these pumps remain operational for 28 days. At the end of the first 28-day period, the pumps were changed to continue the treatment for a total of 56 days. Estrous cyclicity was monitored by daily vaginal lavages. At the end of the experiments, the rats were painlessly killed, the intrabursal location of the cannula's tip was verified by visual inspection, and the ovaries were fixed for either histological analysis or immunohistochemistry (see below).

Immunohistochemistry

After 18–20 h of fixation in Zamboni's fixative, the ovaries were transferred to PBS for 24 h, at 4 C and then to 20% sucrose in PBS for an additional day. Thereafter, they were embedded in OCT compound (Miles, Inc.), frozen on dry ice, and stored at −85 C until cryostat sectioning. Ten-micron sections were subjected to immunohistochemistry for p75 NGFR using monoclonal antibody 192 IgG (41), according to a procedure previously reported (42).

Histology

The ovaries from oil-injected controls, EV-treated rats, and EV-treated rats receiving an intrabursal infusion of NGF Ab + p75 NGFR AS or PIMS were cleaned of adherent fat tissue, immersed in Bouin's fixative solution, embedded in paraffin, serially sectioned at 8 μm, and stained with hematoxylin-eosin as previously reported (1). One ovary per animal was subjected to morphometric analysis. When analyzing the effect of NGF Ab + p75 NGFR AS on estrous cyclicity, the contralateral noninfused ovary was also examined after 56 days of treatment. The incidence of corpora lutea, expressed as the number of corpora lutea per ovary, was used to determine whether ovulation had occurred in the different groups of animals. The numbers of preantral, antral, and atretic follicles were counted in every fifth section, as previously described (1). The sizes of both healthy and atretic antral follicles were also determined. Preantral follicles were defined as follicles without any antral cavity and with two or more layers of granulosa cells. Atretic follicles were defined as those follicles with more than 5% of cells with pyknotic nuclei in the largest cross-section, showing oocyte shrinkage and occasional germinal vesicle breakdown (44, 45). Also included in this group were follicles showing deformation (shrinkage or collapsing) or lacking the oocyte.

Cystic follicles were defined according to criteria proposed previously (23) as those follicles devoid of oocytes, displaying a large antral cavity, an enlarged thecal cell layer, and a thin (most frequently monolayer) granulosa cell compartment containing apparently healthy cells (Fig. 1). Type III follicles were also defined according to the criteria proposed by Brawer and colleagues (46, 47). These follicles are large, devoid of oocytes, contain four or five plicated layers of small, densely packed granulosa cells surrounding a very large antrum, and display a seemingly normal thecal compartment. Type III follicles may represent precystic follicular structures (46, 47). Our observations suggest the existence of a transitional stage between healthy preovulatory follicles and the type III follicles described previously (46, 47). Follicles in this transitional stage share all morphological characteristics previously described for type III follicles, but in addition they contain a healthy oocyte. Figure 1 illustrates the morphological differences observed among normal preovulatory follicles (A), type III follicles with oocyte (B), type III follicles without oocyte (C), and follicular cysts (D).

Statistics

Comparisons between several groups were made using a one-way ANOVA followed by the Student-Neuman-Keuls multiple test for unequal replications. Differences in the incidence of cysts and type III follicles were analyzed using the χ^2 test for the comparison of frequency distributions (48).

Results

Development of ovarian cysts

To define the time course of cyst formation after EV injection, the morphological aspect of the ovary was evaluated at different intervals after administration of the steroid. Seven days after the injection, there was a significant decrease in the number of corpora lutea accompanied by an increase in their size (Figs. 2 and 3). By day 15, the average corpora luteum size remained significantly greater than that on day 0 (Figs. 2 and 3). Thirty days after EV injection, both the number and size of the corpora lutea were significantly decreased (Figs. 2 and 3) compared with those in noninjected,

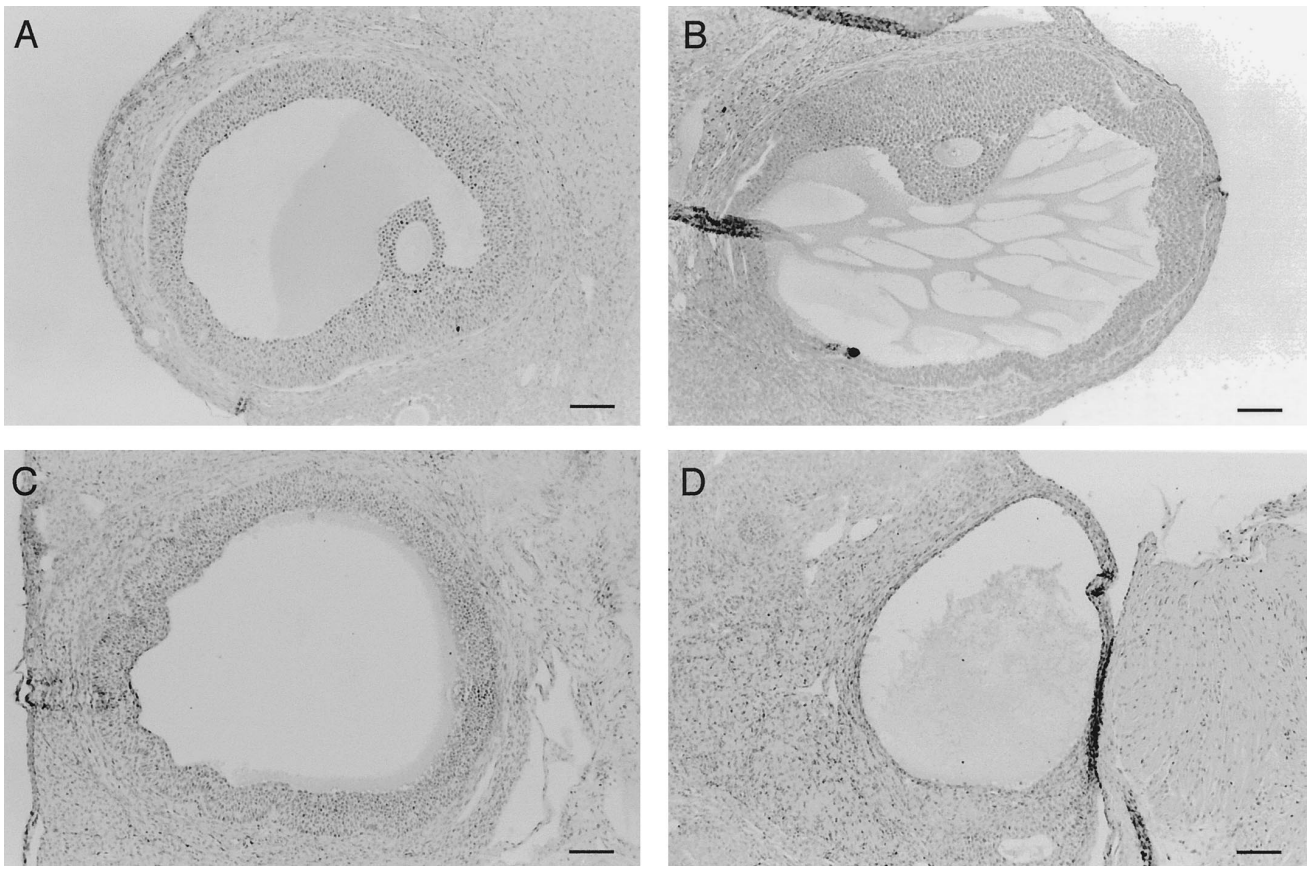

FIG. 1. Morphological aspect of a normal preovulatory follicle (A), a type III follicle containing an oocyte (B), a type III follicle without oocyte (C), and a follicular cyst (D). *Bars*, 100 μm.

day 0 animals. By day 60, corpora lutea were no longer detected in the steroid-treated rats (Figs. 2 and 3). In other experiments, however, corpora lutea were detected at this time in some rats (three of seven rats, two to six corpora lutea per rat).

Although the average size of antral follicles remained similar to that seen in controls throughout the experiment (Fig. 3), type III follicles became apparent for the first time 30 days after EV injection (4 $\pm$ 1.2/ovary; n = 3 rats). By day 60, cystic follicles were also detected. They had an average size of 459 $\pm$ 38 μm (mean $\pm$ SEM; n = 27) and were present at a frequency of 5.2 $\pm$ 1.5/ovary. No luteinized follicles were found. At this time, type III follicles (750 $\pm$ 5 μm; n = 20) were detected at a frequency of 1.1 $\pm$ 0.5/ovary in the ovaries of EV-treated rats. Neither cysts nor type III follicles were detected in the ovaries of untreated rats in this particular group of animals.

Neurotrophin changes in the ovary after EV administration

These experiments were performed to determine whether the changes in NE outflow that occur in the ovary 30 days after EV administration (5) are accompanied by an activation of NGF production in the ovary and/or its low affinity receptor p75 NGFR. This receptor is thought to facilitate the transference of NGF from its sites of production to the innervating fibers (20, 49). Ovarian p75 NGFR mRNA levels, measured by RNase protection assay, increased noticeably after EV administration (Fig. 4A). The first significant increase was observed 15 days postinjection, with values reaching maximal levels by 30 days. At this time, there was a 5-fold increase in message levels with respect to control values; values declined by 60 days, but still remained significantly elevated over control levels. In contrast to p75 NGFR, there was no change in the levels of the mRNA encoding the high affinity NGF receptor, TrkA. NGF mRNA levels, on the other hand, were also increased by EV, but only at 30 days (Fig. 4C), a time at which the NGF mRNA content was 6-fold higher than that in oil-treated controls. Sixty days after EV administration, NGF mRNA values had almost returned to control levels.

These changes in mRNA were correlated with similar changes in NGF and p75 NGFR proteins. Ovarian p75 NGFR content increased significantly over control values by 30 days after EV injection (the earliest interval examined), remaining elevated by 60 days (Fig. 4B). NGF content increased 2-fold by 30 days (Fig. 4D), decreasing to intermediate values thereafter.

EV administration activates noradrenergic neuronal output

The prevertebral celiac ganglion is a prominent site of noradrenergic neurons innervating the ovary (16, 24). To determine whether EV administration affects the activity of noradrenergic neurons in the celiac ganglion and whether such changes precede and/or accompany the appearance of

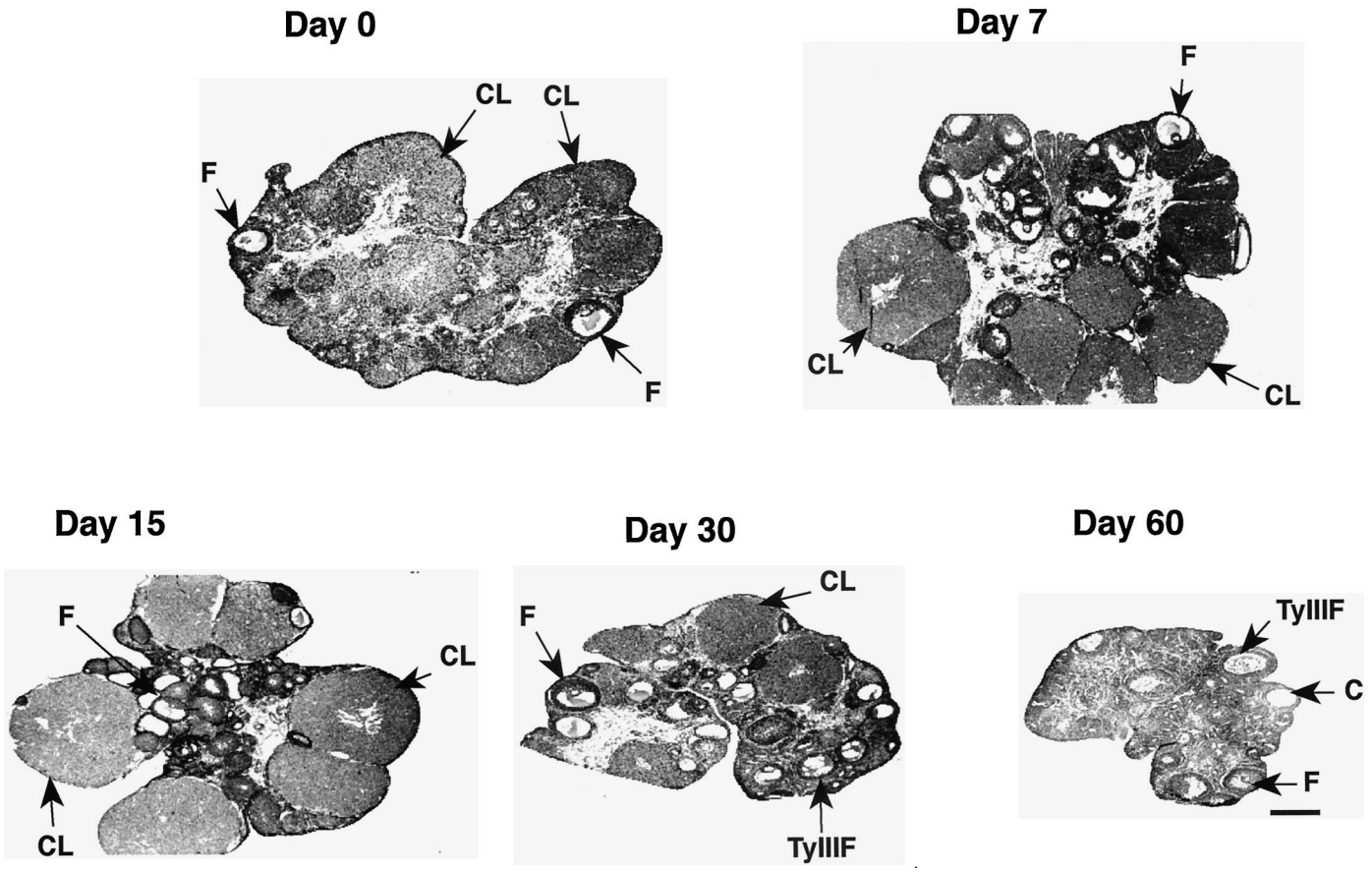

FIG. 2. Morphological aspect of ovaries from adult rats at different intervals after a single sc injection of estradiol valerate. CL, Corpus luteum; F, antral follicle; C, cyst; TyIIIF, type III follicle. *Bar*, 500 μm.

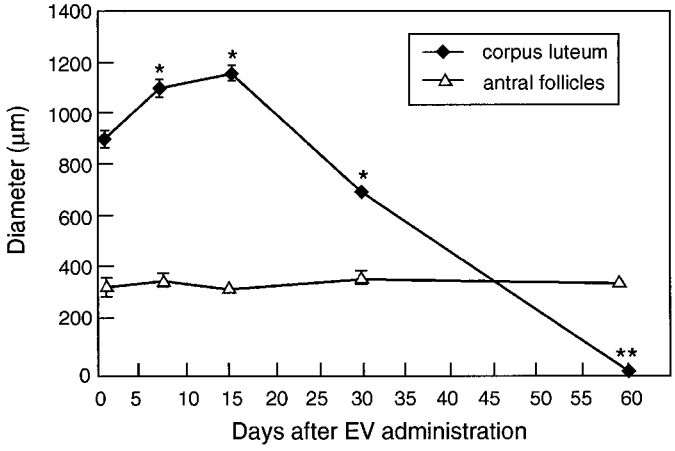

FIG. 3. Changes in the size of corpora lutea and antral follicles in the ovaries of adult rats at different intervals after a single sc injection of EV. Each *point* represents the mean ± SEM of three or four rats. *, $P < 0.01$; **, $P < 0.005$ (*vs.* noninjected, day 0 controls).

ovarian cysts, TH mRNA content was measured 30 and 60 days after EV injection. The results demonstrated that TH mRNA levels were modestly, but significantly, increased at both time points (Fig. 5, *upper panel*). In contrast to these changes in TH mRNA levels, TH activity in the ganglion decreased markedly 30 days after EV, returning to basal values by 60 days (Fig. 5, *middle panel*). As ovarian TH activity increases at these same intervals after EV injection (5), the possibility was considered that the drop in TH activity in the ganglion is related to an increase in axonal transport of the enzyme to the nerve terminals. TH is transported to nerve endings by slow axonal transport (50). Measurement of β-tubulin type IV (RBT_2) mRNA levels as an indirect index of axonal transport (29, 30) demonstrated a substantial increase in RBT_2 mRNA content in the celiac ganglion (Fig. 5, *lower panel*) at the two intervals examined after EV injection. The increase was more prominent 30 days after EV (4-fold), but was still clearly evident by 60 days (3-fold).

Additional experiments using a combination of hybridization histochemistry and retrograde tracing were conducted to more precisely define whether, in addition to the generalized increase in TH mRNA found in the celiac ganglion, an increase specific to the neurons projecting to the ovary also occurs in animals treated with EV. Ten days after the intraovarian administration of fluorogold, celiac ganglion sections were hybridized with the same TH cRNA probe employed for RNase protection assays and examined under darkfield/fluorescent illumination. Numerous TH mRNA-containing neurons were detected, some of which were also fluorogold positive (Fig. 6, *upper panels*). Computerized assessment of cellular TH mRNA levels (determined by the number of silver grains per cell) was used to estimate the relative changes in TH mRNA abundance per cell in control and EV-treated groups. As some of the cells were also

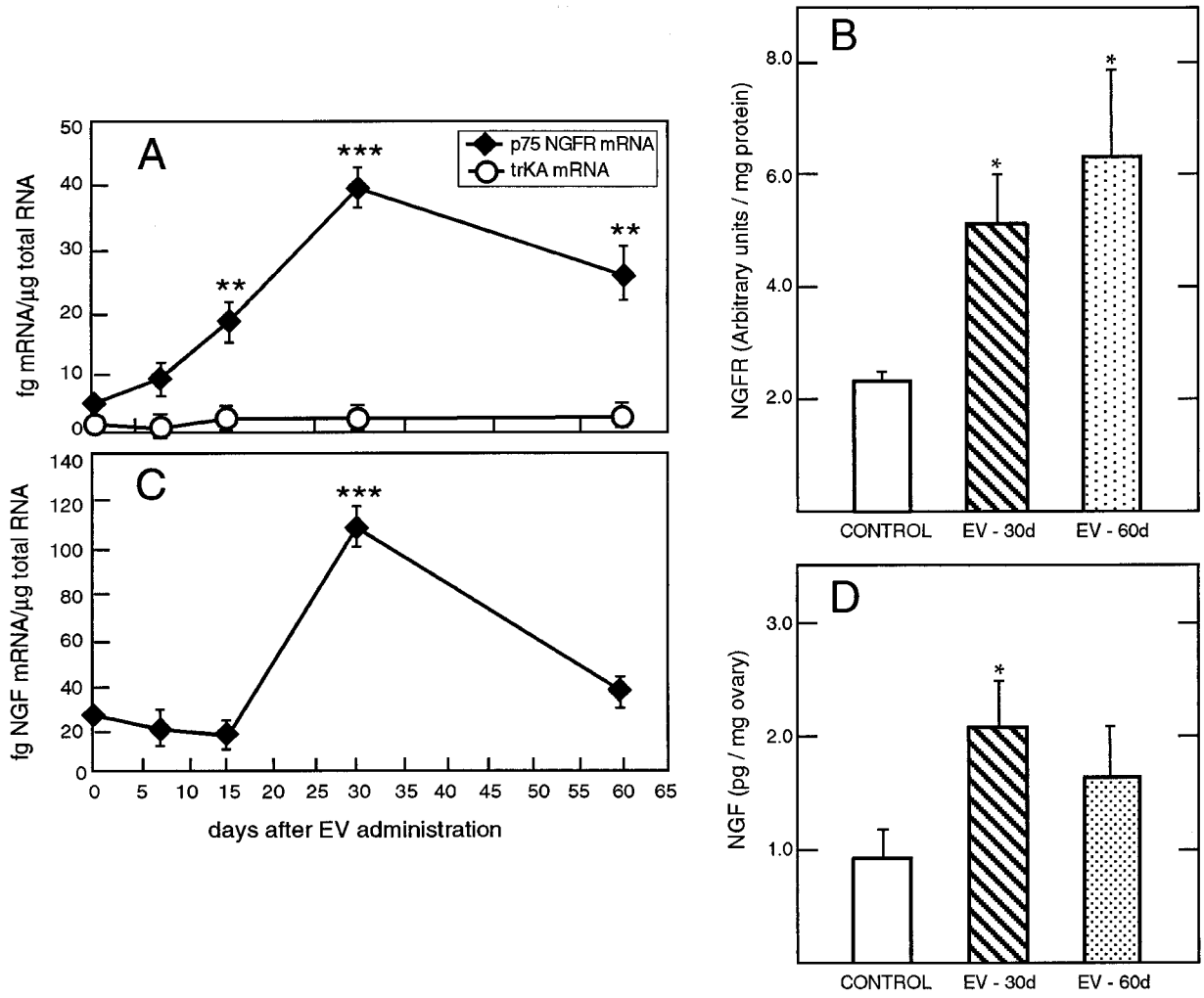

FIG. 4. Changes in the content of p75 NGFR and TrkA mRNA (A), p75 NGFR protein (B), NGF mRNA (C), and NGF protein (D) in the ovaries of adult rats at different intervals after a single injection of EV. The mRNAs were measured by RNase protection assay, p75 NGFR was determined by quantitation of autoradiograms from immunoprecipitated cross-linked [^{125}I]NGF-receptor complexes separated by SDS-PAGE, and NGF was measured by two-site fluorometric enzyme immunoassay. Each *point* or *bar* represents the mean ± SEM of five independent observations (two ovaries per sample). *, $P < 0.05$; **, $P < 0.02$; ***, $P < 0.001$ (*vs.* control day 0).

fluorescent (indicating that they innervate the ovary), it was possible to assess differences in TH mRNA levels between cells innervating the ovary and those sending their axons elsewhere. All measurements were made 30 days after EV administration, *i.e.* before the appearance of cysts. In agreement with the results of the RNase protection assays, we found that EV treatment resulted in a small, but significant ($P < 0.05$), increase in TH mRNA content in catecholaminergic cells not projecting to the ovary (Fig. 6, *lower panel*). A much more robust (40%; $P < 0.01$) increase in TH mRNA content was observed in catecholaminergic cells projecting to the ovary (*i.e.* cells containing both TH mRNA and fluorogold; Fig. 6, *lower panel*).

Reestablishment of ovulatory capacity in EV-treated rats via ovary-specific blockade of NGF and p75 NGFR actions

These experiments were carried out to define the importance of ovarian NGF and its low affinity receptor in the process by which EV induces formation of cysts and leads to loss of estrous cyclicity and ovulatory capacity. Most of the rats receiving an intraovarian infusion of NGF Ab + p75 NGFR AS remained in constant estrus during the first 28 days of infusion (Fig. 7, *upper panel*). Continuation of the infusion for an additional 28-day period by replacement of the minipump with a fresh mixture of inhibitors led to the initiation of irregular estrous cyclicity in four of seven animals (Fig. 7, *upper panel*). Control EV-treated animals receiving an infusion of PIMS behaved like noninfused EV-treated rats, *i.e.* remained in constant estrus throughout the duration of the experiment (Fig. 7, *lower panel*). Infusion of NGF Ab + p75 NGFR AS for only the first 28 days after EV injection failed to restore estrous cyclicity in all eight rats, whereas initiation of the infusion 30 days after EV resulted in restoration of estrous cyclicity in four of eight animals (not shown). As in the case of the prolonged 56-day treatment (Fig. 7), the pattern of estrous cyclicity in these short term treated rats did not have the regularity of that in normal animals.

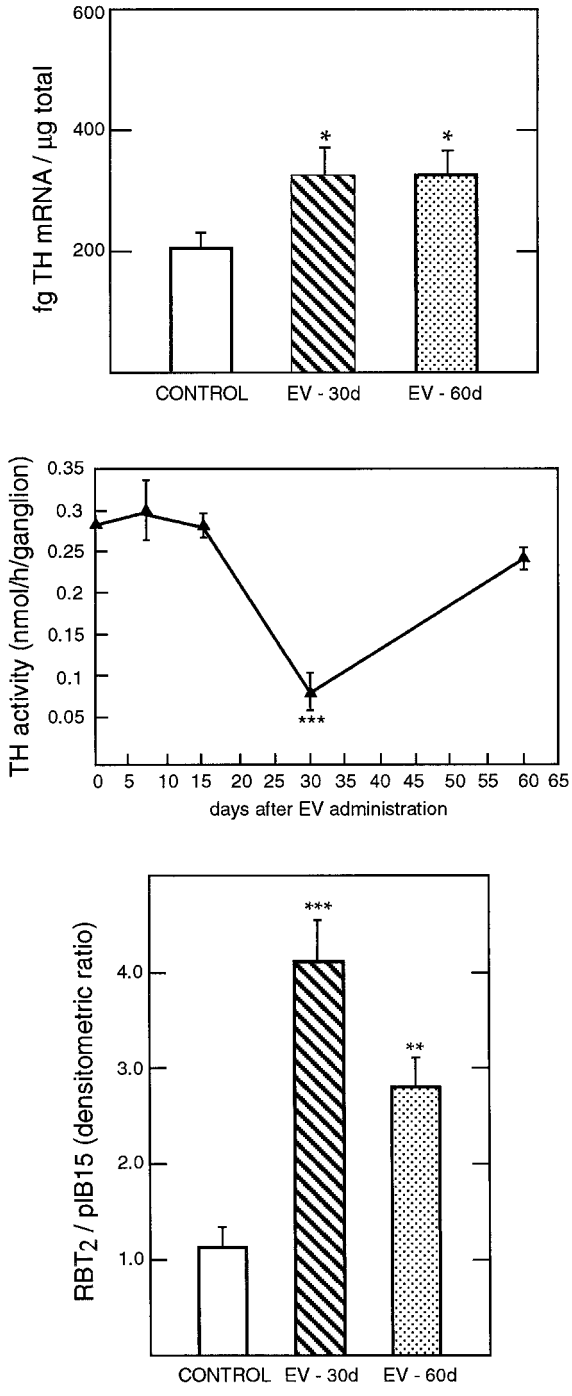

FIG. 5. *Upper panel*, Changes in TH mRNA levels in the celiac ganglion of adult rats 30 (EV-30) and 60 (EV-60) days after a single injection of EV. Each *bar* represents the mean ± SEM of four or five independent observations (two ganglia per observation). *, $P < 0.05$ *vs.* control (day 0). *Middle panel*, Changes in TH activity in the celiac ganglion after EV administration. TH activity is expressed as nanomoles of CO_2 formed per h/ganglion. Each *point* represents the mean ± SEM of four to six independent observations. ***, $P < 0.01$ *vs.* day 0. *Lower panel*, Increase in β-tubulin class IV mRNA (RBT_2) levels in the celiac ganglion after EV administration. Results are presented as the ratio between the constitutively expressed cyclophilin mRNA (p1B15) and β-tubulin class IV mRNA levels, expressed as arbitrary densitometric units. Each *bar* represents the mean ± SEM of four or five independent observations. **, $P < 0.02$; ***, $P < 0.01$ (*vs.* control day 0).

Morphological examination of the ovaries from long term infused rats demonstrated that ovulation had occurred in the EV-treated animals that responded with restoration of estrous cyclicity to the infusion of NGF Ab + p75 NGFR AS. Figure 8 illustrates these findings. Figure 8A shows the ovary from a normal cycling adult rat. Figure 8B shows the ovary of an EV-treated rat infused with PIMS. Figure 8C demonstrates the presence of corpora lutea in the ovary of a rat treated with EV and infused with the NGF Ab + p75 NGFR AS solution.

Morphometric analysis revealed that both the EV injection alone and the blockade of NGF/p75 NGFR actions in EV-treated rats had pronounced effects on the number of antral follicles per ovary. Although EV injection reduced the total number of antral follicles (*i.e.* healthy plus atretic; Fig. 9A), infusion of NGF Ab + p75 NGFR AS reversed this effect, resulting in a number of antral follicles per ovary similar to that in control untreated rats (Fig. 9A). These changes were not particular to either healthy or atretic antral follicles, as the number of both types of follicles decreased with EV and increased toward control values after blockade of NGF/p75 NGFR actions (Fig. 9, B and C). Likewise, they were observed in both rats that responded to the NGF Ab + p75 NGFR AS treatment with restoration of cyclicity and those that remained in constant estrous (see Fig. 7). No changes in the number of preantral follicles were detected with either treatment (not shown). As observed in initial experiments (Fig. 3), EV injection followed by PIMS infusion did not significantly increase the average size of healthy antral follicles (Fig. 9D). Infusion of NGF Ab + p75 NGFR AS was also without effect. EV-treated rats showed a small increase in the size of atretic antral follicles (from 299 ± 15 to 361 ± 27 μm), a change that was obliterated by the inhibition of NGF/p75 NGFR actions (301 ± 27 μm; Fig. 9E). Importantly, the ovaries from EV-treated animals that reinitiated estrous cyclicity after infusion with NGF Ab + p75 NGFR AS (see Fig. 7) had a greater number of corpora lutea than rats treated with EV and infused with PIMS (13.3 ± 4.4 *vs.* 3.8 ± 1.7; Fig. 9F). The contralateral, noninfused ovaries showed similar differences (not shown).

Blockade of NGF/p75 NGFR actions resulted in a significant reduction in the incidence of cysts with respect to that in EV-injected rats infused with PIMS (Table 1). Surprisingly, five of the six untreated controls also had cysts, but at a frequency much lower than that in EV-treated rats and similar to that detected in NGF Ab + p75 NGFR AS-treated rats (Table 1). In addition to reducing the incidence of follicular cysts, blockade of NGF/p75 NGFR actions eliminated type III follicles (Table 1), making the overall follicular population of the ovary similar to that in untreated rats.

Immunohistochemical examination of the ovaries demonstrated an abundance of p75 NGFR-immunoreactive material in both the thecal compartment (Fig. 10A) and nerve fibers (Fig. 10A1) of ovaries from EV-treated rats infused with PIMS. Thecal p75 NGFR immunoreactivity was decreased in ovaries infused with NGF Ab + p75 NGFR AS (Fig. 10B). In contrast to this effect on thecal cells, the infusion was ineffective in decreasing the levels of p75 NGFR immunoreactivity in ovarian nerves (Fig. 10, A1 and B1).

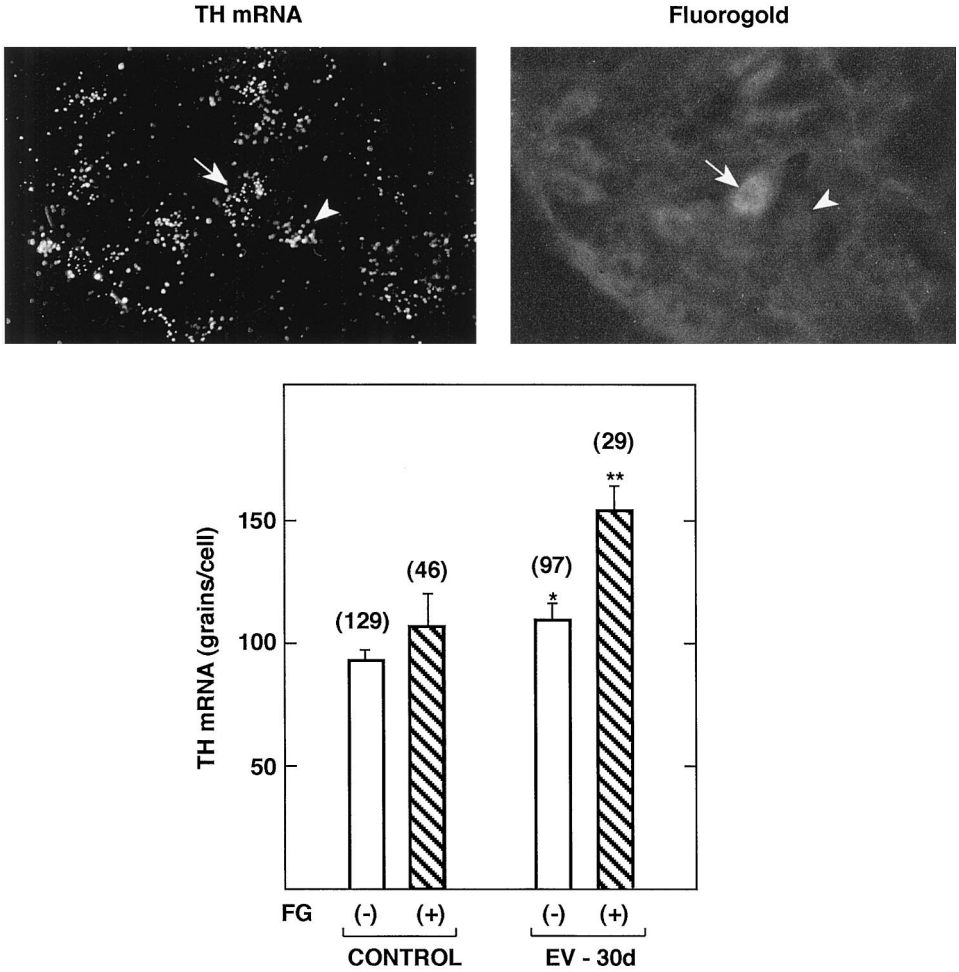

FIG. 6. *Upper panel*, Microphotographs illustrating the identification of catecholaminergic neurons projecting to the ovary from the celiac ganglion by combined *in situ* hybridization-retrograde fluorescent tracing. The ganglia were processed for hybridization histochemistry 10 days after intraovarian injection of the retrograde tracer, fluorogold. The tracer was injected 30 days after the animals had received a single injection of EV. Cells containing TH mRNA alone (*arrowhead*), fluorogold alone (not shown), and both TH mRNA and fluorogold (*arrow*) were visualized under darkfield/UV fluorescent illumination. Double-labeled cells were considered as projecting to the ovary, based on the assumption that the fluorogold previously injected into the ovary was taken up by nerve terminals of innervating neurons and transported by retrograde flow to their perikarya. *Lower panel*, Preferential increase in TH mRNA content in noradrenergic coeliac ganglion neurons projecting to the ovary after EV treatment, as determined by the number of silver grains per cell detected in sections hybridized with a [^{35}S]UTP-labeled TH cRNA probe. *Open bars*, Neurons not projecting to the ovary, *i.e.* fluorogold (FG) negative (−); *hatched bars*, neurons projecting to the ovary, *i.e.* FG positive (+). Numbers in *parentheses* represent the number of cells analyzed. Each *bar* represents the mean ± SEM number of grains per cell. *, $P < 0.05$ *vs.* oil-injected, FG (−) controls; **, $P < 0.01$ *vs.* FG (+) oil-injected controls.

Discussion

The present results demonstrate that 1) the development of ovarian follicular cysts induced by administration of a single dose of EV to rats is preceded by an increased synthesis of NGF and its low affinity receptors in the ovary, and by a selective activation of the celiac ganglion noradrenergic neurons innervating the gland; and 2) intraovarian blockade of NGF actions restores the population of normal antral follicles depleted by EV, reduces the number of precystic and cystic follicles, and restores estrous cyclicity and ovulatory capacity in a majority of animals. These findings suggest that hyperactivation of the ovarian sympathetic input caused by EV is related to an overproduction of NGF and its low affinity receptor in the ovary, and that an enhanced activity of this neurotrophic-neurogenic regulatory system contributes to the process by which EV induces ovarian cysts and disrupts ovulation in rats.

Hallmarks of the polycystic ovarian syndrome, the most common endocrine disorder of women in reproductive age (8, 51), are the presence of multiple, medium-sized, nonatretic, antral follicles in the ovary (6) and augmented androgen secretion (6, 51–53). To date, an animal model that thoroughly mimics all of the abnormalities underlying the human pathology has not been described. Nevertheless, administration of a single injection of EV to adult rats has been shown to reproduce several of the ovarian abnormalities in PCOS, including the formation of ovarian cysts, hyperthecosis, and increased androgen production in addition to anovulation and loss of estrous cyclicity (17, 23, 46). Using this rodent model, an alteration of the neurogenic control of the ovary, inferentially suspected by others to contribute to the human syndrome (11, 14), was found to be a distinct component of the EV-induced ovarian pathology (5, 17). Specifically, these studies showed that preceding the appearance of the cysts, there was an activation of the sympathetic innervation to the ovary, as revealed by an increased release of newly incorporated NE from ovarian nerves, augmented ovarian NE content and TH enzymatic activity, and enhanced incorporation of labeled NE into ovarian tissue (5). That this abnormally high sympathetic activity contributes to maintaining the anovulatory state in EV-treated animals was indicated by the prompt resumption of cyclicity and ovulatory capacity in animals subjected to transection of the superior ovarian nerve (17), the main source of sympathetic fibers innervating ovarian follicles (16).

EV may enhance peripheral sympathetic activity by acting on neuronal systems that directly (16, 24) or transsynaptically innervate the ovary (54, 55) and/or on the ovarian system of target-derived trophic factors that supports the sympathetic innervation of the gland (56). Without contesting the poten-

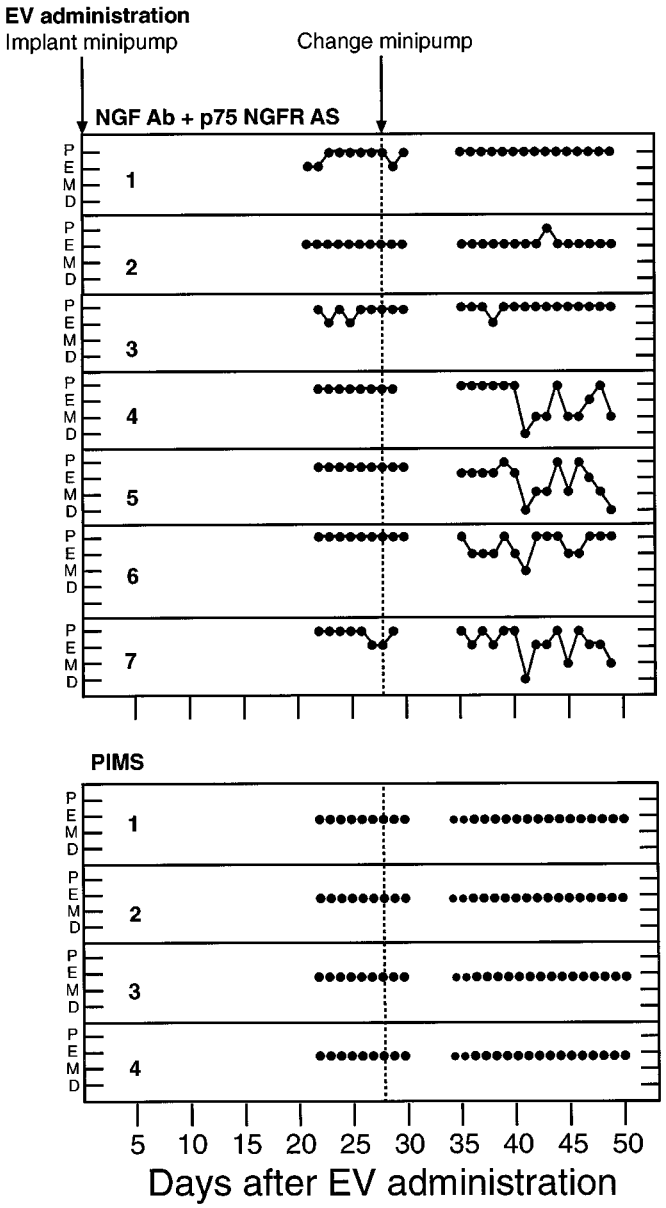

FIG. 7. Partial restoration of estrous cyclicity in EV-treated rats by the intrabursal infusion of NGF antibodies (NGF Ab) and a p75 NGFR antisense mRNA oligodeoxynucleotide (p75 NGFR AS) administered via Alzet osmotic minipumps (Alza Corp.). Control animals were infused with PIMS. The pumps were implanted at the time of the EV injection and were replaced after 28 days with a new pump containing fresh inhibitors. The gaps in each estrous cycle profile denote periods when vaginal lavages were not collected. To show both responders and nonresponders all seven animals infused with NGF Ab + p75 NGFR AS are represented. To improve the clarity of the illustration only four of five controls are shown. The animal not shown had a profile identical to the other four. P, Proestrus; E, estrous; M, diestrous day 1; D, diestrous day 2.

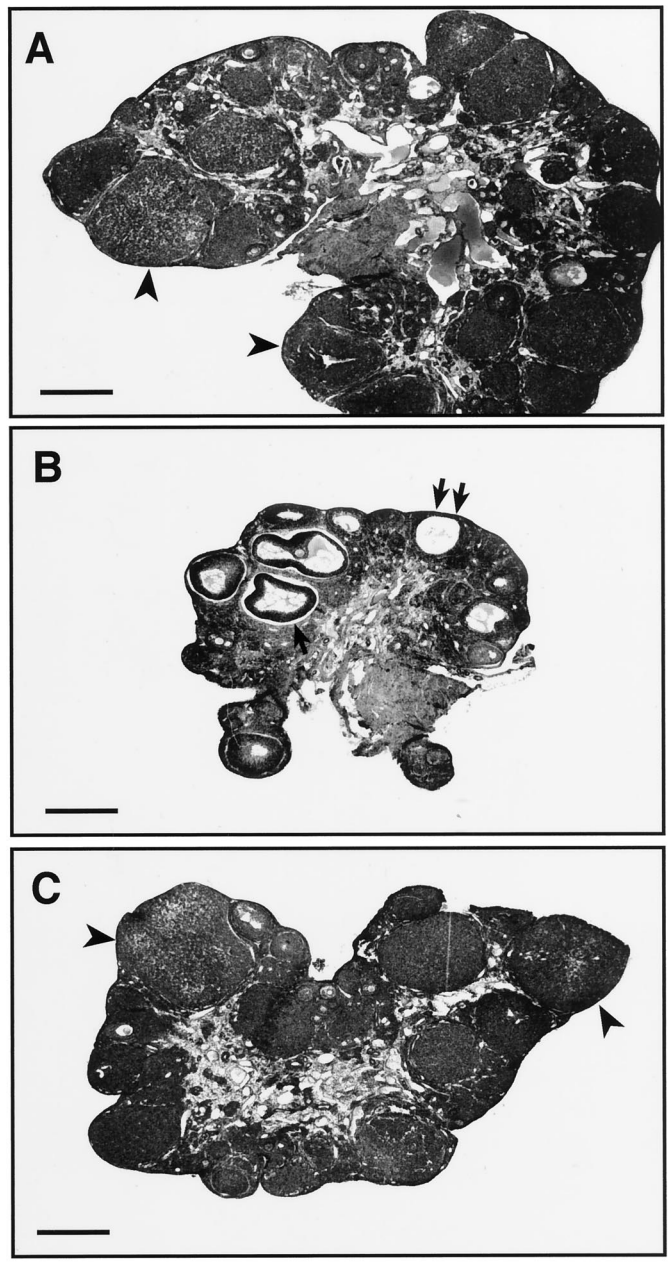

FIG. 8. Morphological aspect of the ovary from an untreated normal rat (A), an animal treated with EV and infused with PIMS (B), and an animal treated with EV and infused with a mixture of NGF Ab + p75 NGFR AS for 56 days (C). Notice that the ovary receiving this infusion ovulated, as indicated by the presence of corpora lutea (*arrowheads*). The ovary of an animal receiving the control infusion (B) does not show signs of ovulation and instead contains antral follicles (*arrow*) and follicular cysts (*double arrows*). *Bars*, 560 μm.

tial importance of the former site of action, the present results suggest the existence of the latter. Together, they support two related concepts: 1) that the increased noradrenergic flow to the ovary observed in animals with EV-induced cystic ovary (5) is, to a significant extent, caused by an increased production of NGF and the low affinity p75 NGFR in the ovary; and 2) that a deranged expression of this neurotrophic signaling complex is an integral component of the mechanism by which EV induces anovulation in rats.

Although EV-induced follicular cysts become first detected around 60 days after the EV injection (Ref. 46 and this study), activation of the sympathetic innervation to the ovary precedes the formation of follicular cysts by at least a month (5). In turn, synthesis of p75 NGFR increases as early as 15 days after EV administration and is followed shortly by

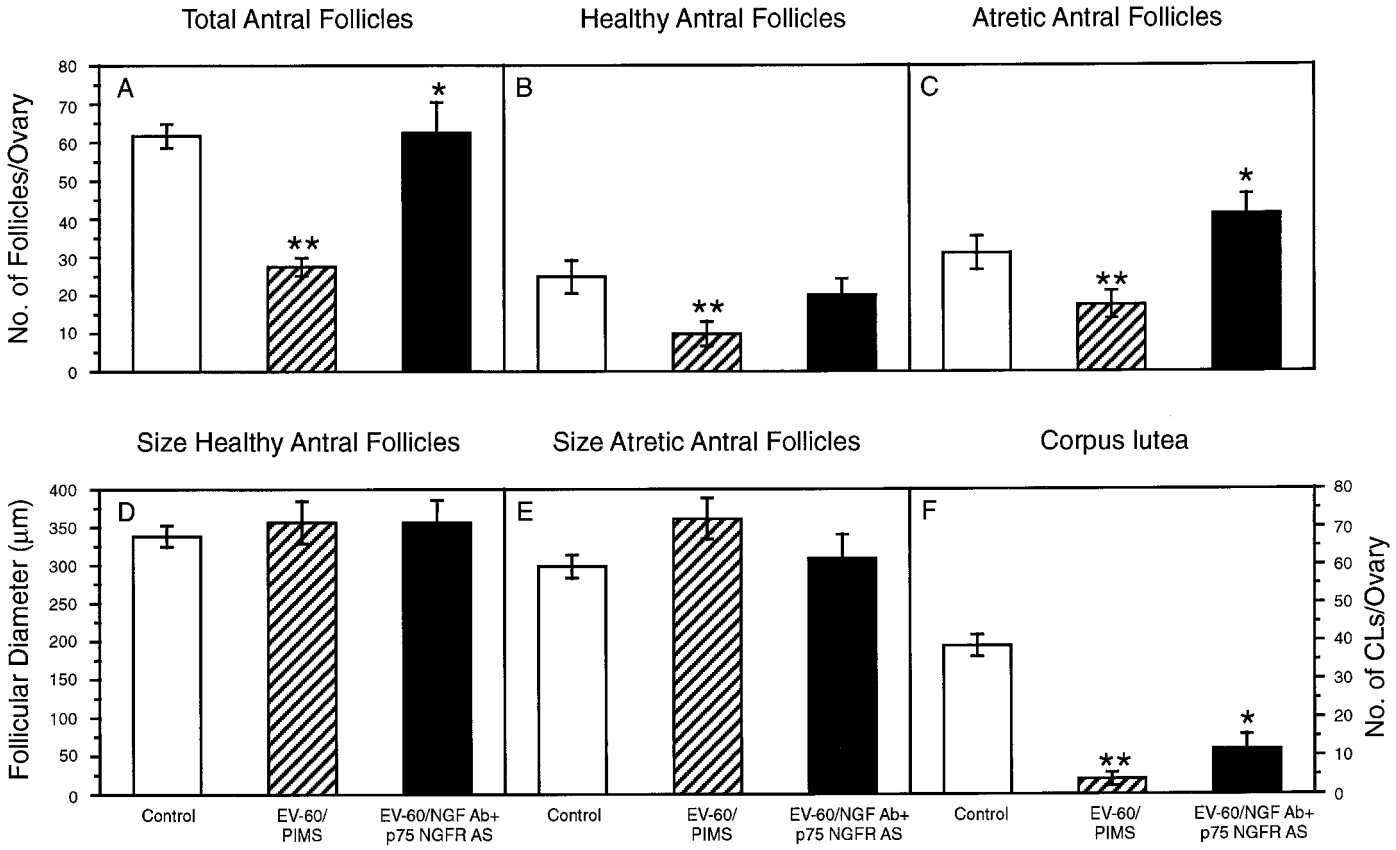

FIG. 9. Effect of blocking intraovarian NGF/p75 NGFR actions in EV-treated rats on the total number of antral follicles per ovary (A), the number of healthy antral follicles (B), the number of atretic antral follicles (C), the size of healthy antral follicles (D), the size of atretic antral follicles (E), and ovulation (F), as assessed by the number of corpora lutea per ovary. Control, Untreated rats (n = 6); EV-56/PIMS, EV-treated animals infused intrabursally with PIMS for 56 days (n = 5); EV-56/NGF Ab + p75 NGFR AS, EV-treated rats infused intrabursally with antibodies to NGF plus an antisense deoxyoligonucleotide against p75 NGFR for 56 days (n = 6, except for corpora lutea data where n = 4). *, $P < 0.05$ *vs.* EV-56/PIMS treated group; **, $P < 0.05$ *vs.* control groups.

TABLE 1. Incidence of follicular cysts and type III follicles (Ty III F) in untreated rats, EV-treated rats infused intrabursally with preimmune serum (PIMS), and EV-treated rats infused intrabursally with a mixture of NGF antibodies and an antisense oligonucleotide to p75 NGFR to reduce NGF/p75 NGFR actions

Ovarian structure	Groups		
	Untreated control (n = 6)	EV-56d,[a] PIMS-infused[b] (n = 5)	EV-56d, NGF Ab + p75 NGFR AS infused[b,c] (n = 4)
Total no. of cysts/total no. of healthy antral follicles	11/184	26/50	10/66[d]
Cyst size (μm)	385 ± 36[e]	459 ± 38	408 ± 47
Total no. of Ty III F/total no. of healthy antral follicles	0/184	6/50	0/66[d]
Ty III F size (μm)		739 ± 27	

[a] Estradiol valerate, administered as a single im injection (2 mg/rat on day 0).
[b] Infused intrabursally via Alzet osmotic minipumps for 56 days beginning on the day of EV injection.
[c] This group only includes the rats that responded to the infusion with NGF Ab plus p75 NGFR AS with reinitiation of estrous cyclicity (see Fig. 7).
[d] $P < 0.01$ *vs.* EV-56d/PIMS-infused ovaries and not different from untreated controls (by χ^2 test).
[e] Mean ± SEM.

augmentation of NGF synthesis, indicating that activation of this ligand/receptor module is an early event in the process by which EV administration disrupts ovarian function. An increased neurotrophic support to the sympathetic neurons projecting to the ovary is likely to play a significant role in enhancing the sympathetic outflow to the ovary in EV-treated rats. TH mRNA levels were selectively augmented in noradrenergic celiac neurons projecting to the ovary, an effect that can hardly be attributed to estrogen itself, as the steroid inhibits, rather than stimulates, TH synthesis (38, 57, 58). In contrast, NGF is a potent inducer of both TH gene expression (59, 60) and TH enzymatic activity (59, 61). In the ovary, NGF and both of its receptors, p75 NGFR and the high affinity TrkA tyrosine kinase receptor, are synthesized in thecal cells (19, 42), a prominent terminal field of the sympathetic neurons innervating the ovary (42, 62, 63). Neonatal

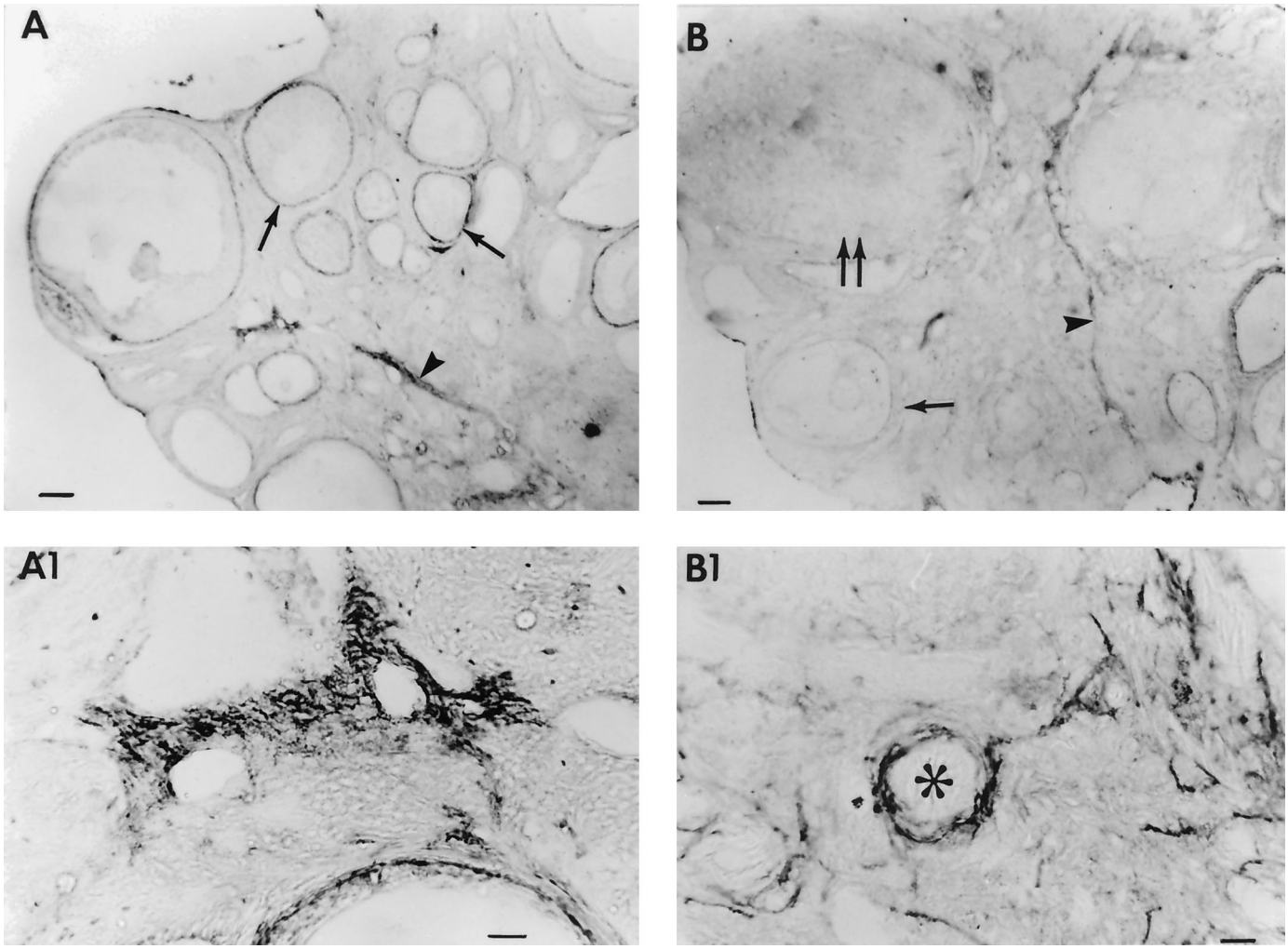

FIG. 10. Decreased p75 NGFR immunoreactivity in the thecal compartment of ovaries from EV-treated rats after the intraovarian infusion of a mixture of NGF Ab and p75 NGFR AS via Alzet osmotic minipumps (Alza Corp.) administered for 56 days after EV injection. A, p75 NGFR immunoreactivity is located in the thecal compartment of antral follicles (*arrows*) and nerve fibers (*arrowhead*). B, Ovary from an EV-treated rat infused with NGF Ab + p75 NGFR AS. Notice the presence of a corpus luteum (*double arrows*), the decreased content of p75 NGFR-immunoreactive material in the thecal compartment of antral follicles (*single arrow*), and the seemingly normal intensity of p75 NGFR immunoreactivity in nerve fibers (*arrowhead*). *Bars*, 100 μm. A1, Higher magnification view of the ovary from an EV-treated rat infused with PIMS, depicting the presence of p75 NGFR immunoreactivity in a bundle of nerve fibers. B1, Similar view of an ovary from an EV-treated rat infused with NGF Ab + p75 NGFR AS, showing the apparently normal content of p75 NGFR in nerve fibers. *, Blood vessel. *Bars*, 20 μm.

immunoneutralization of NGF actions inhibits the development of ovarian sympathetic innervation and delays follicular growth (1), highlighting both the critical importance of the trophic factor in supporting the innervation of the ovary and the facilitatory role of sympathetic nerves on follicular development.

The early activation of ovarian p75 NGFR synthesis after EV suggests that there is also an early increase in NGF availability to the innervating neurons. The p75 NGFR not only facilitates transfer of NGF from its sites of production to NGF-sensitive fibers (20, 64), but can collaborate with the high affinity TrkA receptor to potentiate cellular responses to the neurotrophin (65). The subsequent increase in NGF synthesis detected 30 days after EV would ensure a continuously supply of the polypeptide to the nerve terminals and, hence, to the projecting neurons.

The increase in NGF and p75 NGFR synthesis that follows EV administration raises the question of the mechanism(s) by which EV causes such an increase. Previous studies have shown an increase in ovarian NGF gene expression (19), but not in p75 NGFR (42), in the afternoon and evening of the first proestrus, *i.e.* at the time of the preovulatory surge of gonadotropins. No alterations in either NGF or p75 NGFR mRNA levels were detected at times preceding the LH surge, when plasma estrogen levels are most elevated, suggesting that the preovulatory changes in NGF expression are not due to estrogen *per se*, but to gonadotropins instead. It is doubtful that the dual up-regulatory effect of EV on NGF and p75 NGFR expression is due to an increase in basal gonadotropin release caused by a centrally mediated effect of the steroid. Both plasma LH and FSH levels decrease within 2 weeks after EV injection, remaining below control levels for at least 60 days (15, 23). An EV-dependent defect in the ovarian receptor system mediating LH actions remains a possibility, as trans-

genic animals overexpressing the LH gene develop a PCO-like condition in the absence of any functional changes reflecting LH receptor down-regulation by the inappropriately high plasma LH levels (66). Another possibility is a direct up-regulatory effect of EV on ovarian p75 NGFR and NGF gene expression. Such an effect appears unlikely, as estrogen has been shown to down-regulate, rather than up-regulate, p75 NGFR mRNA levels in other tissues (67). Moreover, we observed that EV injection is followed 24 h later by some increase in p75 NGFR and a marked, but transient, increase in ovarian TrkA mRNA content (coinciding with an ovulatory LH surge), with no change in NGF mRNA levels (data not shown). Thus, there must be an intermediate event responsible for the delayed (7–30 days) p75 NGFR and NGF responses to EV. Further studies are required to resolve this issue.

The intrabursal administration of NGF antibodies and a p75 NGFR AS decreased the incidence of precystic structures (type III follicles) and follicular cysts and reversed, in a majority of animals, the anovulatory condition imposed by EV. This effectiveness strongly suggests that the increase in ovarian NGF and/or p75 NGFR production that follows EV administration is a contributing factor to both the process by which the ovary becomes anovulatory in response to EV, and the mechanism that leads to cyst formation. Supporting this idea is the finding that a 2-fold increase in intraovarian production of NGF, via genetically engineered cells grafted into the ovaries of otherwise normal animals, disrupted estrous cyclicity and resulted in an increased incidence of precystic type III follicles (68).

Two potential mechanisms may underlie the recovery of ovulatory capacity that follows attenuation of NGF/p75 NGFR function in EV-treated rats. One is a reduction in the abnormally high sympathetic tone to the ovary, as transection of the superior ovarian nerve in EV-treated rats results is a similar recovery (17). The other may involve correction of an exaggerated influence of NGF on follicular homeostasis, as NGF appears to exert a direct effect on follicular growth (69). The increased number of antral follicles and the reduction in precystic and cystic structures observed in the ovaries of EV-treated rats infused with NGF Ab + p75 NGFR AS suggest that in the absence of an abnormal NGF influence, more normal follicles become able to reinitiate growth and eventually succeed in ovulating. This interpretation is supported by the findings presented in the companion paper (68) showing that sustained induction of abnormally high intraovarian NGF levels results in a reduction in the number of antral follicles per ovary and a greater incidence of follicle type III formation. That is, exposure of the ovary to an abnormally high NGF influence leads to alterations in follicular dynamics resembling some of those caused by EV.

The subpopulation of follicles that ovulate in response to the normalization of NGF/neurogenic influences may be recruited not only from normal, antral follicles, but also from transitional type III follicles, *i.e.* those containing a healthy oocyte. Earlier findings indicated that even though type III follicles may represent a precystic condition, they might be the only follicles capable of ovulation in EV-treated rats (46, 47). Type III follicles bind labeled hCG as intensely as a preovulatory follicle and yet do not ovulate or luteinize unless exposed to preovulatory LH levels. As the incidence of type III follicles decreased in rats infused with NGF Ab + p75 NGFR AS and increases in rats subjected to an isolated increase in intraovarian NGF levels (68), it may be inferred that the amelioration of an abnormally increased NGF/p75 NGFR function in EV-treated rats leads to dismissal of these structures via ovulation.

With respect to the hormonal mechanisms responsible for the recovery of ovulatory competence and estrous cyclicity seen in NGF Ab + p75 NGFR-treated rats, a decrease in androgen production, and, consequently, in androgen negative feedback, needs to be considered as a contributing factor. While the ovaries of EV-treated rats exhibit a profound androgenic hyperresponsiveness to both hCG and β-adrenergic stimulation (17), rats carrying intraovarian grafts of NGF-producing cells have elevated serum levels of androstenedione (68). Thus, the normalization of NGF/p75 NGFR function in EV-treated rats may allow restoration of ovulatory capacity by disrupting an abnormal NGF influence on both ovarian androgen output and follicular growth. Not all animals responded to NGF Ab + NGFR AS with restoration of estrous cyclicity and/or ovulation despite showing changes in follicular dynamics similar to those seen in rats that reinitiated cyclicity. This partial recovery may be related to inefficient delivery of the test substances to the ovary and/or to the likely need of correcting the availability of additional factors to achieve full restoration of normal ovarian function.

A surprising observation made in the course of these studies was the recovery of ovulatory capacity of both the ovary infused with NGF Ab + p75 NGFR AS and the contralateral, untreated gland. An early study (47) described a similar phenomenon after hemiovariectomy of rats with EV-induced PCO and implicated an increase in pulsatile LH release in the process by which the remaining ovary became able to ovulate. We infer that in the present study the loss of an abnormally high intraovarian NGF-p75 NGFR signaling activity during the infusion with NGF Ab + p75 NGFR AS results in changes in pulsatile gonadotropin levels able to stimulate both ovaries and thus reverse the anovulatory condition. Support for this idea comes from the finding that hemiovariectomy of EV-treated animals results in an ovulatory rate (47) comparable to that detected in ovaries with inhibited NGF/p75 NGFR function.

In summary, the present results demonstrate the contribution of a target-derived neurotrophic component to the physiopathological process underlying EV-induced PCO in rats. In conjunction with the results presented in the companion paper (68), this study identifies NGF, signaling through the p75 NGFR, as a neurotrophic factor relevant to the process. The potential relationship that this signaling system may have to the intragonadal production of follistatin, a candidate gene product recently identified by linkage analysis as involved in the etiology of human PCOS (9) remains to be determined.

References

1. **Lara HE, McDonald JK, Ojeda SR** 1990 Involvement of nerve growth factor in female sexual development. Endocrinology 126:364–375
2. **Curry Jr TE, Lawrence Jr IE, Burden HW** 1984 Ovarian sympathectomy in the guinea pig. Cell Tissue Res 236:257–263
3. **Adashi EY, Hsueh AJW** 1981 Stimulation of b_2-adrenergic responsiveness by follicle-stimulating hormone in rat granulosa cells *in vitro* and *in vivo*. Endocrinology 108:2170–2178
4. **Aguado LI, Petrovic SL, Ojeda SR** 1982 Ovarian β-adrenergic receptors during the onset of puberty: characterization, distribution, and coupling to steroidogenic responses. Endocrinology 110:1124–1132
5. **Lara HE, Ferruz JL, Luza S, Bustamante DA, Borges Y, Ojeda SR** 1993 Activation of ovarian sympathetic nerves in polycystic ovary syndrome. Endocrinology 133:2690–2695
6. **Franks S** 1995 Polycystic ovary syndrome. N Engl J Med 333:853–861
7. **Lobo RA** 1996 A unifying concept for polycystic ovary syndrome. In: Chang RJ (ed) Polycystic Ovary Syndrome. Springer, New York, pp 334–352
8. **Diamanti-Kandarakis E, Dunaif A** 1996 New perspectives in polycystic ovary syndrome. Trends Endocrinol Metab 7:267–271
9. **Urbanek M, Legro RS, Driscoll DA, Azziz R, Ehrmann DA, Norman RJ, Strauss III JF, Spielman RS, Dunaif A** 1999 Thirty-seven candidate genes for polycystic ovary syndrome: strongest evidence for linkage is with follistatin. Proc Natl Acad Sci USA 96:8573–8578
10. **Erickson GF** 1991 Folliculogenesis in polycystic ovary syndrome. In: Dunaif A, Givens JR, Haseltine FP, Merriam GR (eds) Polycystic Ovary Syndrome. Blackwell Scientific, Boston, pp 111–128
11. **Semenova II** 1969 Adrenergic innervation of ovaries in Stein-Leventhal syndrome. Vestn Akad Med Nauk SSSR 24:58–62
12. **Allen WM, Woolf RB** 1959 Medullary resection of the ovaries in the Stein-Leventhal syndrome. Am J Obstet Gynecol 77:826–837
13. **Katz M, Carr PJ, Cohen BM, Millar RP** 1978 Hormonal effects of wedge resection of polycystic ovaries. Obstet Gynecol 51:437–444
14. **Garcia-Rudaz C, Armando I, Levin G, Escobar ME, Barontini M** 1998 Peripheral catecholamine alterations in adolescents with polycystic ovary syndrome. Clin Endocrinol (Oxf) 49:221–228
15. **Schulster A, Farookhi R, Brawer JR** 1984 Polycystic ovarian condition in estradiol valerate-treated rats: spontaneous changes in characteristic endocrine features. Biol Reprod 31:587–593
16. **Lawrence Jr IE, Burden HW** 1980 The origin of the extrinsic adrenergic innervation to the rat ovary. Anat Rec 196:51–59
17. **Barria A, Leyton V, Ojeda SR, Lara HE** 1993 Ovarian steroidal response to gonadotropins and b-adrenergic stimulation is enhanced in polycystic ovarian syndrome. Role of the sympathetic innervation. Endocrinology 133:2696–2703
18. **Levi-Montalcini R** 1987 The nerve growth factor 35 years later. Science 237:1154–1162
19. **Dissen GA, Hill DF, Costa ME, Dees WL, Lara HE, Ojeda SR** 1996 A role for *trk*A nerve growth factor receptors in mammalian ovulation. Endocrinology 137:198–209
20. **Johnson EMJ, Taniuchi M, DiStefano PS** 1988 Expression and possible function of nerve growth factor receptors on Schwann cells. Trends Neurosci 11:299–304
21. **Lara H, Leyton V, Fiedler JL, Dissen GA, Ojeda SR** 1998 An increase in ovarian neurotrophins contributes to the development of polycystic ovary. Soc Neurosci Abstr 24:2005
22. **Brawer JR, Naftolin F, Martin J, Sonnenschein C** 1978 Effects of a single injection of estradiol valerate on the hypothalamic arcuate nucleus and on reproductive function in the female rat. Endocrinology 103:501–512
23. **Brawer JR, Munoz J, Farookhi R** 1986 Development of the polycystic ovarian condition (PCO) in the estradiol valerate-treated rat. Biol Reprod 35:647–655
24. **Baljet B, Drukker J** 1979 The extrinsic innervation of the abdominal organs in the female rat. Acta Anat 104:243–267
25. **Waymire I, Bjur R, Weiner N** 1971 Assay of tyrosine hydroxylase by coupled decarboxylation of dopa formed from [1-^{14}C]-L-tyrosine. Anal Biochem 43:588–600
26. **Bustamante D, Lara H, Belmar J** 1989 Changes of norepinephrine levels, tyrosine hydroxylase and dopamine-b-hydroxylase activities after castration and testosterone treatment in vas deferens of adult rats. Biol Reprod 40:541–548
27. **Ma YJ, Dissen GA, Rage F, Ojeda SR** 1996 RNase protection assay. Methods: A Companion to Methods in Enzymology 10:273–278
28. **Grima B, Lamouroux A, Blanot F, Faucon Biguet N, Mallet J** 1985 Complete coding sequence of rat tyrosine hydroxylase mRNA. Proc Natl Acad Sci USA 82:617–621
29. **Bond JF, Robinson GS, Farmer SR** 1984 Differential expression of two neural cell-specific beta-tubulin mRNAs during rat brain development. Mol Cell Biol 4:1313–1319
30. **Ginzburg I, Teichman A, Dodemont HJ, Behar L, Littauer UZ** 1985 Regulation of three b-tubulin mRNAs during rat brain development. EMBO J 4:3667–3673
31. **Whittemore SR, Friedman PL, Larhammar D, Persson H, Gonzalez-Carvajal M, Holets VR** 1988 Rat β-nerve growth factor sequence and site of synthesis in the adult hippocampus. J Neurosci Res 20:403–410
32. **Radeke MJ, Misko TP, Hsu C, Herzenberg LA, Shooter EM** 1987 Gene transfer and molecular cloning of the rat nerve growth factor receptor. Nature 325:593–597
33. **Danielson PE, Forss-Petter S, Brow MA, Calavetta L, Douglass J, Milner RJ, Sutcliffe JG** 1988 p1B15: a cDNA clone of the rat mRNA encoding cyclophilin. DNA 7:261–267
34. **Dissen GA, Newman Hirshfield A, Malamed S, Ojeda SR** 1995 Expression of neurotrophins and their receptors in the mammalian ovary is developmentally regulated: Changes at the time of folliculogenesis. Endocrinology 136:4681–4692
35. **Simmons DM, Arriza JL, Swanson LW** 1989 A complete protocol for *in situ* hybridization of messenger RNAs in brain and other tissues with radiolabeled single-stranded RNA probes. J Histotechnol 12:169–181
36. **Berg-von der Emde K, Dees WL, Hiney JK, Hill DF, Dissen GA, Costa ME, Moholt-Siebert M, Ojeda SR** 1995 Neurotrophins and the neuroendocrine brain: different neurotrophins sustain anatomically and functionally segregated subsets of hypothalamic dopaminergic neurons. J Neurosci 15:4223–4237
37. **Schmued L, Fallon JH** 1986 Fluoro-gold: a new fluorescent retrograde axonal tracer with numerous unique properties. Brain Res 377:147–154
38. **Kohama SG, Bethea CL** 1995 Steroid regulation of tyrosine hydroxylase messenger ribonucleic acid in dopaminergic subpopulations of monkey hypothalamus. Endocrinology 136:1790–1800
39. **Korsching S, Thoenen H** 1987 Two-site enzyme immunoassay for nerve growth factor. Methods Enzymol 147:167–185
40. **Lara HE, Hill DF, Katz KH, Ojeda SR** 1990 The gene encoding nerve growth factor is expressed in the immature rat ovary: effect of denervation and hormonal treatment. Endocrinology 126:357–363
41. **Taniuchi M, Johnson Jr EM** 1985 Characterization of the binding properties, and retrograde axonal transport of a monoclonal antibody directed against the rat nerve growth factor receptor. J Cell Biol 101:1100–1106
42. **Dissen GA, Hill DF, Costa ME, Ma YJ, Ojeda SR** 1991 Nerve growth factor receptors in the peripubertal rat ovary. Mol Endocrinol 5:1642–1650
43. **Sariola H, Saarma M, Sainio K, Arumäe U, Palgi J, Vaahtokari A, Thesleff I** 1991 Dependence of kidney morphogenesis on the expression of nerve growth factor receptor. Science 254:571–573
44. **Hirshfield AN** 1988 Size-frequency analysis of atresia in cycling rats. Biol Reprod 38:1181–1188
45. **Hirshfield AN, Midgley AR** 1978 Morphometric analysis of follicular development in the rat. Biol Reprod 19:597–605
46. **Brawer J, Richard M, Farookhi R** 1989 Pattern of human chorionic gonadotropin binding in the polycystic ovary. Am J Obstet Gynecol 161:474–480
47. **Convery M, McCarthy GF, Brawer JR** 1990 Remission of the polycystic ovarian condition (PCO) in the rat following hemiovariectomy. Anat Rec 226:328–336
48. **Zar JH** 1984 Biostatistical Analysis, ed. 2. Englewood Cliffs, NJ: Prentice Hall,
49. **Wyatt S, Shooter EM, Davies AM** 1990 Expression of the NGF receptor gene in sensory neurons and their cutaneous targets prior to and during innervation. Neuron 2:421–427
50. **Grafstein B, Forman DS** 1980 Intracellular transport in neurons. Physiol Rev 60:1167–1283
51. **Franks S** 1997 Polycystic ovary syndrome: Approaching the millennium. Hum Reprod 12:43–45
52. **Yen SSC** 1991 Chronic anovulation caused by peripheral endocrine disorders. In: Yen SSC, Jaffe RB (eds) Reproductive Endocrinology: Physiology, Pathophysiology and Clinical Management, vol 3. WB Saunders, Philadelphia, pp 576–630
53. **Ehrmann DA, Barnes RB, Rosenfield RL** 1995 Polycystic ovary syndrome as a form of functional ovarian hyperandrogenism due to dysregulation of androgen secretion. Endocr Rev 16:322–353
54. **Kawakami M, Kubo K, Uemura T, Nagase M, Hayashi R** 1981 Involvement of ovarian innervation in steroid secretion. Endocrinology 109:136–145
55. **Marchetti B, Cioni M, Scapagnini U** 1985 Ovarian LHRH receptors increase following lesions of the major LHRH structures in the rat brain: involvement of a direct neural pathway. Neuroendocrinology 41:321–331
56. **Ojeda SR, Dissen GA, Malamed S, Hirshfield AN** 1994 A role for neurotrophic factors in ovarian development. In: Hsueh AJW, Schomberg DW (eds) Ovarian Cell Interactions: Genes to Physiology. Springer-Verlag, New York, pp 181–202
57. **Morrell JI, Rosenthal MF, McCabe JT, Harrington CA, Chikaraishi DM, Pfaff DW** 1989 Tyrosine hydroxylase mRNA in the neurons of the tuberoinfundibular region and zona incerta examined after gonadal steroid hormone treatment. Mol Endocrinol 3:1426–1433
58. **Blum M, McEwen BS, Roberts JL** 1987 Transcriptional analysis of tyrosine hydroxylase gene expression in the tuberoinfundibular dopaminergic neurons of the rat arcuate nucleus after estrogen treatment. J Biol Chem 262:817–821
59. **Thoenen H, Barde Y-A** 1980 Physiology of nerve growth factor. Physiol Rev 60:1284–1334
60. **Gizang-Ginsberg E, Ziff EB** 1990 Nerve growth factor regulates tyrosine hydroxylase gene transcription through a nucleoprotein complex that contains c-Fos. Genes Dev 4:477–491
61. **Hefti F, Gnahn H, Schwab ME, Thoenen H** 1982 Induction of tyrosine hydroxylase by nerve growth factor and by elevated K^+ concentrations in cultures of of dissociated sympathetic neurons. J Neurosci 2:1554–1566

62. **Burden HW** 1985 The adrenergic innervation of mammalian ovaries. In: Ben-Jonathan N, Bahr JM, Weiner RI (eds) Catecholamines as Hormone Regulators. Raven Press, New York, pp 261–278
63. **Papka RE, Cotton JP, Traurig HH** 1985 Comparative distribution of neuropeptide tyrosine-, vasoactive intestinal polypeptide-, substance P-immunoreactive, acetylcholinesterase-positive and noradrenergic nerves in the reproductive tract of the female rat. Cell Tissue Res 242:475–490
64. **Chao MV, Hempstead BL** 1995 p75 and Trk: A two-receptor system. Trends Neurosci 18:321–326
65. **Hantzopoulos PA, Suri C, Glass DJ, Goldfard MP, Yancopoulos GD** 1994 The low affinity NGF receptor, p75, can collaborate with each of the trks to potentiate functional responses to the neurotrophins. Neuron 13:187–201
66. **Risma KA, Hirshfield AN, Nilson JH** 1997 Elevated luteinizing hormone in prepubertal transgenic mice causes hyperandrogenemia, precocious puberty, and substantial ovarian pathology. Endocrinology 138:3540–3547
67. **Sohrabji F, Miranda RC, Toran-Allerand CD** 1994 Estrogen differentially regulates estrogen and nerve growth factor receptor mRNAs in adult sensory neurons. J Neurosci 14:459–471
68. **Dissen GA, Lara HE, Leyton V, Paredes A, Hill DF, Costa ME, Martínez-Serrano A, Ojeda SR** 2000 Intraovarian excess of nerve growth factor increases androgen secretion and disrupts estrous cyclicity in the rat. Endocrinology 141:1073–1082
69. **Ojeda SR, Romero C, Tapia V, Dissen GA**, Neurotrophic and cell-cell dependent control of early follicular development. Mol Cell Biol, in press